Journal of Applied Polymer Science

Determination of the Si—H Content of Hydrogen Silicone Oil by a Combination of the Fourier Transform Near Infrared, Attenuated Total Reflectance-Fourier Transform Infrared, and Partial Least Squares Regression Models

Qianqian Zhai, Shigui Zhao, Chuanjian Zhou, Wenjie Li, Cun Peng
School of Materials Science and Engineering, Shandong University, Jinan 250061, People's Republic of China
Correspondence to: S. Zhao (E-mail: zhaoshigui@sdu.edu.cn)

ABSTRACT: To verify the feasibility of the determination of the Si—H content (HC) of hydrogen silicone oil (HS-oil) with Fourier transform near infrared (FT-NIR) spectroscopy and attenuated total reflectance (ATR)–Fourier transform infrared (FTIR) spectroscopy combined with the partial least squares regression (PLS-R) model, HS-oil samples were synthesized from concentrated hydrosilicone oil (HC = 1.4 wt %), octamethylcyclotetrasiloxane, and hexamethyldisiloxane or prepared by the dilution of concentrated hydrosilicone oil with octamethylcyclotetrasiloxane. The FT-NIR PLS-R model (8695–4000 cm^{-1}, two principal components) was developed from the FT-NIR spectral data, and the coefficient of determination for cross-validation (R^2) and the coefficient of determination for external validation (r^2) were 0.992 and 0.995, respectively. The ATR–FTIR PLS-R model (2302–2040 cm^{-1}, one principal component) was developed from the ATR–FTIR spectral data; it produced an R^2 of 0.995 and an r^2 of 0.996. This study demonstrated that the combination of FT-NIR and ATR–FTIR spectroscopy with the PLS-R model were successfully used to determine the HC of the HS-oil. © 2014 Wiley Periodicals, Inc. J. Appl. Polym. Sci. **2014**, *131*, 40694.

KEYWORDS: oil and gas; spectroscopy; theory and modeling

Received 17 December 2013; accepted 6 March 2014
DOI: 10.1002/app.40694

INTRODUCTION

Hydrogen silicone oil (HS-oil) is an important organic silicon polymer because of its nontoxic, noncorrosive, odorless, and nonflammable properties. It can be used for waterproofing, mold release, defoaming, lubrication, and other applications, in which the Si—H bond is very active and frequently used for the combination of other organic polymer chains with organosilicon via hydrosilylation. So, the amount of Si—H or the Si—H content (HC) is an important index for its application. The chemical method,[1] namely, iodometry, is the most used method for measuring the HC of HS-oil. However, it is not only costly but also polluting and time-consuming, and the procedure is tedious. So, the iodometry method does not meet the requirement of the rapid determination of bulk samples.

In the ASTM definition, *near infrared* (NIR) refers to electromagnetic wavelength from 780 to 2526 nm,[2] and it was the first nonvisible light that humans discoverd.[3] NIR absorption bands are mainly combination bands and overtones of the fundamental vibrations of C—H, N—H, and O—H groups in the mid infrared (MIR) area. The absorption of NIR energy by organic groups is much weaker than the comparable absorption of MIR energy; this enables the analysis of multicomponent samples in a nondestructive way without complicated pretreatments. The use of multivariate statistical methods, such as partial least squares regression (PLS-R), principal component analysis, multiple linear regression, and principal component regression, provides the possibility of establishing a relationship (i.e., calibration models) between the NIR spectral data and the structural or component information of materials.

Over the years, the use of NIR spectroscopy combined with multivariate statistical methods has increased rapidly because of its advantages, including its nondestructiveness, rapidity, nonpolluting nature, and convenience. A number of studies has demonstrated that NIR can be used for the determination of the contents of water, protein, starch, fat, and so on in agricultural products and food production[4–18] and other areas of life.[19,20] NIR has also been applied for the measurement of aspirin, water, alkaloid contents, and so on in medicines;[21–24] the quantification of the octane value, density, refractive index, and so on in the petrochemical field;[25–28] and the determination of hydroxyl group and monomer conversion, particle size, molar

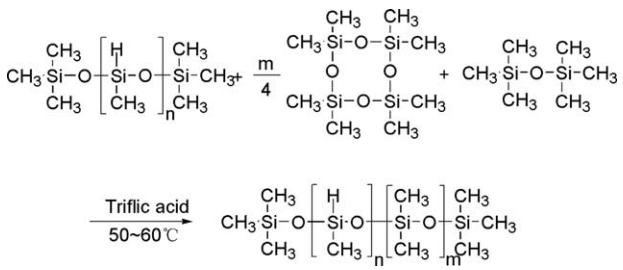

Figure 1. Reaction equations for the preparation of HS-oil samples with various HCs.

ratio, molecular weight, polymerization degree, and so on in the macromolecular field.[29–37] In comparison, MIR spectroscopy combined with multivariate statistical methods has also been used in quantification analysis.[12,29,38,39]

In this study, the feasibility of using Fourier transform near infrared (FT-NIR) diffuse reflectance spectroscopy and attenuated total reflectance(ATR)–Fourier transform infrared (FTIR) spectroscopy combined with the PLS-R model to determine the HCs of HS-oil samples was investigated.

EXPERIMENTAL

Materials

Concentrated hydrosilicone oil (industrial grade, HC = 1.4 wt %) was purchased from Jinan Ruiyuan Chemical Reagent Co. (Jinan, China). Octamethylcyclotetrasiloxane (D_4; chemically pure reagent) was supplied by Jinan Great Chemical Reagent Co. (Jinan, China). Hexamethyldisiloxane (MM; chemically pure reagent) was obtained from Jinan Great Chemical Reagent Co. (Jinan, China). Trifluoromethane sulfonic acid (analytical reagent) was purchased from Aladdin Reagent Co. (Shanghai, China). NH_4HCO_3 (analytical reagent) was purchased from Tianjin Guangcheng Chemical Reagent Co. (Tianjin, China).

Preparation of the HS-Oil Samples[1]

Twenty-one HS-oil samples with different HCs (samples 1–13 and 50–57) were synthesized at 50–60° centigrade from concentrated hydrosilicone oil, D_4, and MM. The mixture was heated with trifluoromethane sulfonic acid for 6 h (see Figure 1). The trifluoromethane sulfonic acid was neutralized with NH_4HCO_3, and the low-boiling-point components were removed *in vacuo*. There was a chemical equilibrium between the break and the formation of the Si—O bonds under acidic conditions, and the break of the Si—O bond in MM and D_4 was much faster than in concentrated hydrosilicone oil with a long-chain structure. In contrast, the driving force of the formation of Si—O bonds in the long-chain structure was much bigger than in the cyclic and short-chain structures. So, the overall trend of the reaction was that the structure $[—Si(CH_3)_2O—]_4$ resulting from the ring opening of D_4 connected to the long chain of the concentrated hydrosilicone oil with MM as the end-capping reagent.

The reference method for HC determination was the standard iodometry method.[1] HS-oil samples 14–49 were prepared by the dilution of samples 1–13 with D_4.

Collection of the FT-NIR and ATR–FTIR Spectra

FT-NIR spectra (spectral resolution = 4 cm^{-1}, wave-number range = 12,000–4000 cm^{-1}, gold was the standard reference, 16 scans) were recorded at ambient temperature with an FT-NIR

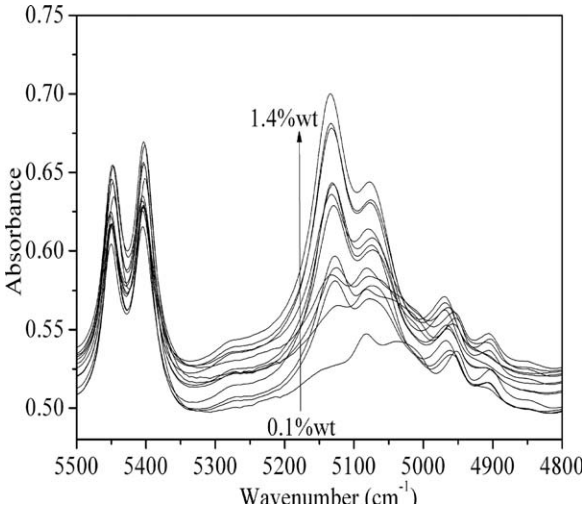

Figure 3. FT-NIR spectra of HS-oil samples 1–13 (5500–4800 cm^{-1}).

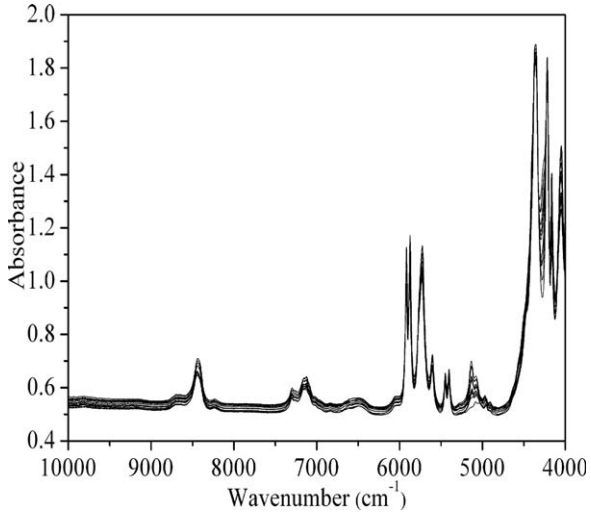

Figure 2. FT-NIR spectra of HS-oil samples 1–13 (10,000–4000 cm^{-1}).

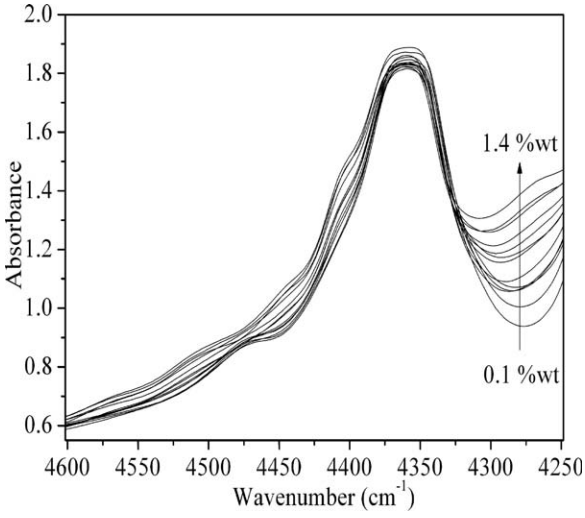

Figure 4. FT-NIR spectra of HS-oil samples 1–13 (4600–4250 cm^{-1}).

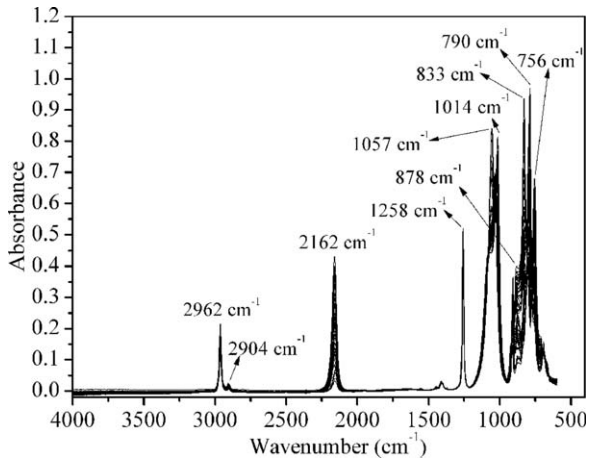

Figure 5. ATR–FTIR spectra of HS-oil samples 1–49 (4000–600 cm^{-1}).

spectrometer (TENSOR 37, Bruker Optics China) operated in diffuse reflection mode. To get the NIR spectra, the samples were put into a cuvette (outer diameter = 22 mm) together with a diffuse reflecting device with precise spacers; this resulted in an optical path length of 2 mm. An NIR integrating sphere was used to collect reflected energy from a spherical perspective and, thereby, captured a complete and quantitative response from the sample. Each sample was measured separately four times to minimize deviation.

ATR–FTIR spectra (spectral resolution: 4 cm^{-1}, wave-number range = 4000–400 cm^{-1}, 16 scans) were collected with MIRacle single-reflection horizontal ATR with ZnSe crystals (Bruker Optics China, incident angle = 45°). Each sample was measured once.

Calibration Model Development

Multivariate statistical analysis was performed with The Unscrambler 9.7 software. The FT-NIR spectra and ATR–FTIR spectra of the samples were imported into The Unscrambler as dependent variables. The HCs of the samples were imported as independent variables. All 57 samples were divided into calibration set samples (samples 1–49) to develop the PLS-R models and the external validation samples (samples 50–57) to validate the PLS-R models. The HCs all ranged from 0.1 to 1.4 wt %.

The FT-NIR spectra of the calibration set samples with high-frequency noises ranging from 8696 to 4000 cm^{-1} removed and without preprocessing were used to develop the FT-NIR PLS-R model. The ATR–FTIR spectra of the characteristic absorption of the Si—H stretching vibrations of the calibration set samples ranging from 2302 to 2040 cm^{-1} were used to develop the ATR–FTIR PLS-R model.

The cross-validation procedure was introduced to the development of the PLS-R models; this means one sample was left out to be used as the prediction set each time, and the other 48 samples were used as the calibration set for the PLS-R model. Then, the HC of the left out sample was predicted by the model on the basis of the calibration set. The procedure was automatically repeated by the software from the first sample to the last one to test whether the model would be obviously affected by the removal of the left out sample.

The PLS-R models were assessed by the coefficient of determination for the cross-validation (R^2), defined with eq. (1), and the root mean square error of cross-validation (RMSE), defined with eq. (2). In a regression model, R^2 is the numerical coefficient that expresses the link between the variation in the predictors and the variation in the response. It is used to indicate the fit of the data. RMSE is a measurement of the average difference between the predicted and measured values, and it also can be interpreted as the average modeling error:

$$R^2 = \left(1 - \frac{\sum_{i=1}^{i=n} (y_{is} - y_{ip})^2}{\sum_{i=1}^{i=n} (y_{is} - y_n)^2}\right) \quad (1)$$

$$\mathrm{RMSE} = \sqrt{\frac{\sum_{i=1}^{i=n} (y_{is} - y_{ip})^2}{n}} \quad (2)$$

where y_{is} and y_{ip} are the HCs of the calibration sample i obtained by standard iodometry and the PLS-R model, respectively; n is the number of samples; and y_n is the average of the HCs obtained by standard iodometry. The regression coefficients of the calibration model show the regions of the spectrum that correlated with HC. The optimal number of principal components was determined in a function of the first local minimum in the RMSE curve, and the prediction was calculated with the optimal principal components.

External Validate of the Calibration Model

The external validation set samples 50–57 were not included in the calibration model and were used to validate the calibration models. The FT-NIR and ATR–FTIR spectral data of these samples were collected under the same conditions with the calibration set samples; each sample was measured once. The predicted results were evaluated by the coefficient of determination for the external validation (r^2) and the root mean square error for the external validation (RMSEEV).

RESULTS AND DISCUSSION

FT-NIR and ATR–FTIR Spectra

NIR absorption bands are associated with the combination and overtone bands of the fundamental MIR vibrations of the

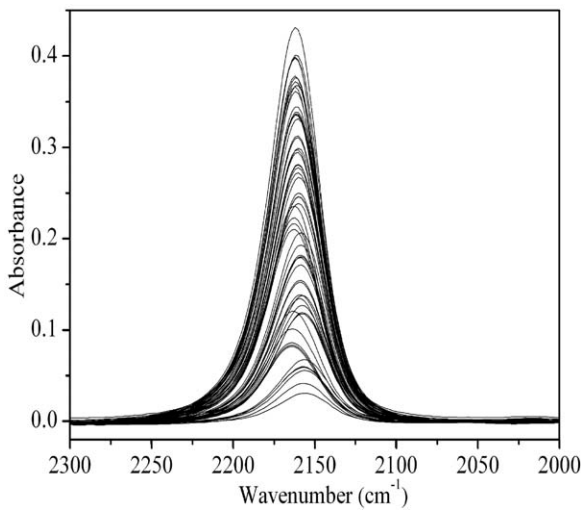

Figure 6. ATR–FTIR spectra of HS-oil samples 1–49 (2300–2000 cm^{-1}).

Table I. Model Statistics for the Cross-Validation and External Validation of the HCs in the HS-Oil Samples

Model	Parameters of cross-validation								Parameters of external validation		
	N^a	Number of principal components	Wave-number range (cm^{-1})	R^2	RMSE (wt %)	SEC[b]	Bias (wt %)[c]	Offset (wt %)[d]	n^e	r^2	RMSEEV (wt %)
FT-NIR model	49	2	8696–4000	0.992	0.0342	0.0343	0.0001	0.0066	8	0.995	0.0226
ATR-FTIR model	49	1	2302–2040	0.995	0.0286	0.0289	0.0003	0.0048	8	0.996	0.0189

[a] *N*, number of calibration set samples.
[b] SEC, standard error of cross -validation.
[c] Systematic difference between the predicted and measured values.
[d] Point at which a regression line crosses the ordinate (*y* axis).
[e] *n*, number of external set samples.

hydric groups, such as C—H, O—H, S—H, and N—H. HS-oil contains many Si—H and C—H groups, and their absorptions are located at different wave numbers in the NIR region. The ratio of Si—H and C—H varies in HS-oil samples with different HCs, which can be reflected in NIR spectra. There are subtle differences, although the NIR spectra of all of the samples were quite similar, as shown in Figure 2. The absorption in 5500–4800 (Figure 3) and 4600–4250 cm^{-1} (Figure 4) increased obviously with increasing HC. Figure 5 shows the full-range ATR–FTIR spectra of the HS-oil samples. The peak at 2162 cm^{-1}, without being overlapped, represented the Si—H stretching vibration, which also increased with increasing HC, and is shown more clearly in Figure 6 from 2300 to 2000 cm^{-1}. There was a certain level of band shift due to the different chemical environments of the Si—H bonds, which resulted from the uncontrolled distribution of Si—H groups but within a reasonable range.[1] The peak at 2962 and 2904 cm^{-1} represented the stretching vibrations of C—H from Si—CH_3, and that at 1258 cm^{-1} was associated with the symmetric deformation vibrations of Si—CH_3. The peaks at 1057 and 1014 cm^{-1} were assigned to the stretching vibrations of Si—O. The peak at 878 cm^{-1} was attributed to the bending vibrations of Si—H. The peaks at 833 and 765 cm^{-1} belonged to the rocking vibrations of —CH_3 from Si—Me_2 and Si—Me, respectively. The peak at 791 cm^{-1} was assigned to the stretching vibrations of Si—C.[1] So, the HS-oils were successfully synthesized.

Calibration Models

Model statistics of the measured and predicted values of the cross-validation results of the HCs are presented in Table I. The R^2 values of the FT-NIR PLS-R model and ATR–FTIR PLS-R model were pretty high, more than 0.99; this showed a good fit of the data. The RMSEs of both models were very low, smaller than 0.035 wt %. Figures 7 and 8 show the performance of the FT-NIR PLS-R model (two principal components) and ATR–FTIR PLS-R model (one principal component) for cross-validation. NIR absorption bands are associated with the combination and overtone bands. The absorption band of Si—H was hardly to find. As a result, a broad wave-number range, with high-frequency noise from 8696 to 4000 cm^{-1} removed, was chosen to develop the FT-

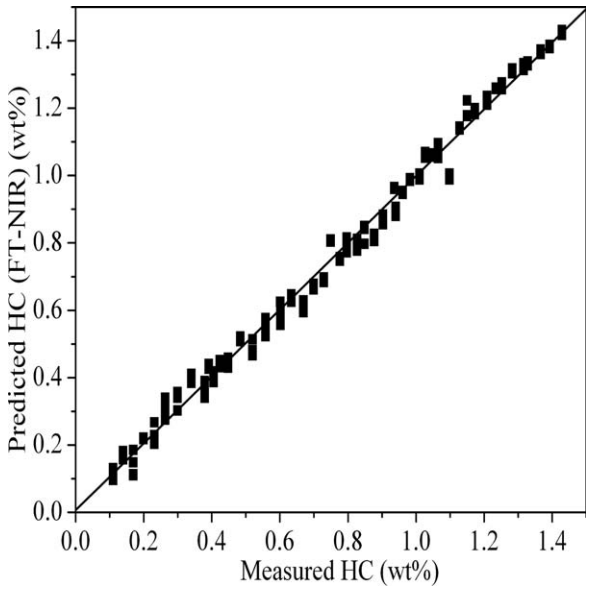

Figure 7. Measured HCs versus predicted HCs for calibration set samples 1–49 by the FT-NIR PLS-R model (cross-validation).

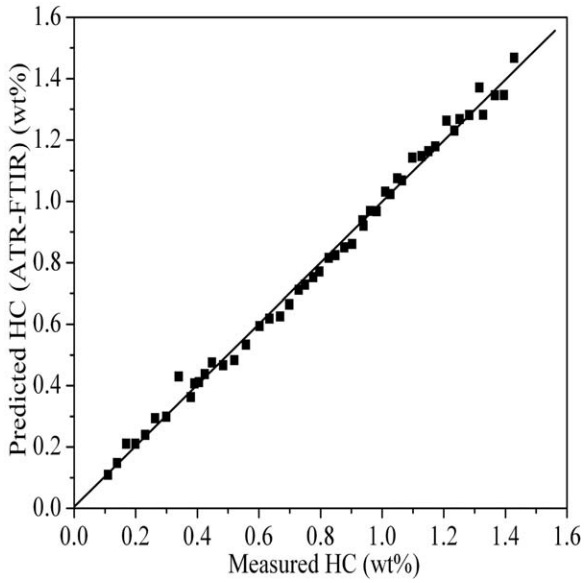

Figure 8. Measured HCs versus predicted HCs for calibration set samples 1–49 by the ATR–FTIR PLS-R model (cross-validation).

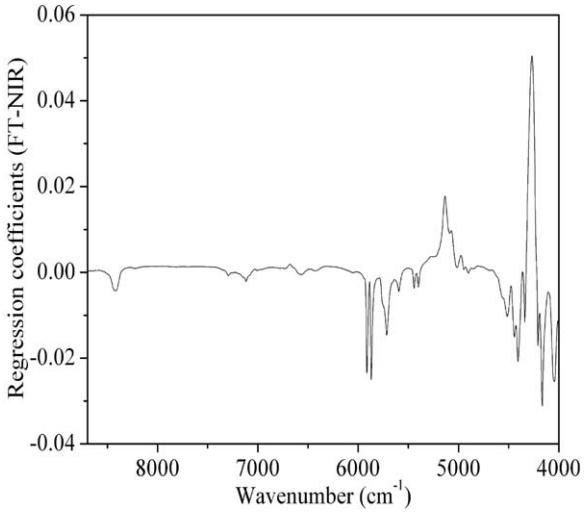

Figure 9. Regression coefficients of the FT-NIR PLS-R model for the HCs of HS-oil.

NIR PLS-R model. But in the MIR area, the absorption band of Si—H was associated with the peak at 2162 cm^{-1}, so, a narrow wave-number range from 2302 to 2040 cm^{-1} was used to develop the ATR–FTIR PLS-R model, and the high R^2 indicated that the band shifts had little impact on the model. Compared to the FT-NIR PLS-R model with two principal components, the ATR–FTIR PLS-R model with only one principal component had the higher R^2, and the lower RMSE, that is, because the FT-NIR PLS-R model was based on a broader wave-number range. This may have consisted of some useless information, whereas the ATR–FTIR PLS-R model was based on the only one absorption peak, which represented exactly the stretching vibrations of Si—H.

Figures 9 and 10 indicate the regression coefficients of the absorption intensities at the wave numbers that the FT-NIR (8696–4000 cm^{-1}) and ATR–FTIR (2302–2040 cm^{-1}) PLS-R models were based on. In Figure 9, the ranges 5500–4800 and 4600–4250 cm^{-1}, which express the obvious differences in Figures 3 and 4, showed positive regression coefficients, respectively. This was likely because the absorption bands of Si—H were in these two ranges. The C—H of the HS-oil displayed a negative correlation in the remaining wave-number range. As shown in Figure 10, there was only one positive peak in the range 2302–2040 cm^{-1}, where the exact absorption peak of Si—H stretching was (shown in Figure 6), and this showed a positive regression coefficient.

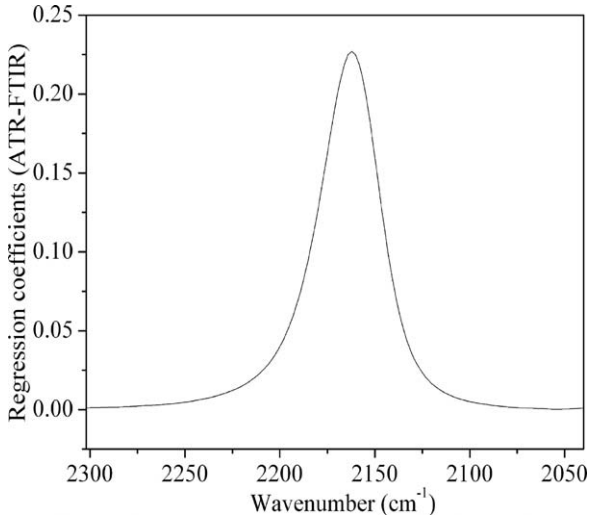

Figure 10. Regression coefficients of the ATR–FTIR PLS-R model for the HCs of HS-oil.

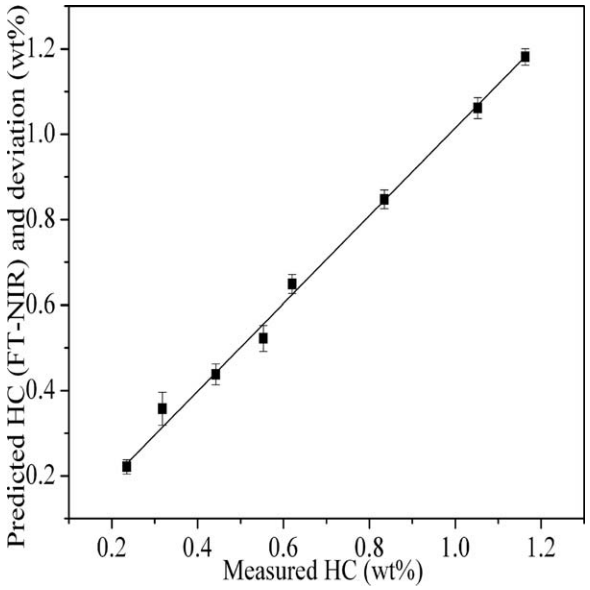

Figure 11. Measured HCs versus predicted HCs for external validation set samples 50–57 by the FT-NIR PLS-R model

External Validation of the Calibration Models

The external validation set of samples 50–57 were used to validate the previous two PLS-R models; the HCs of these samples were previously determined by standard iodometry and ranged

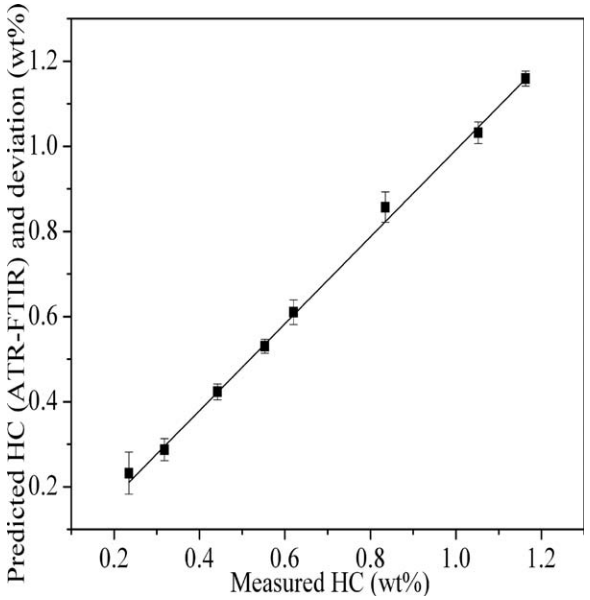

Figure 12. Measured HCs versus predicted HCs for external validation set samples 50–57 by the ATR–FTIR PLS-R model.

from 0.199 to 1.157 wt %. The measured versus predicted values of the HCs with deviation are shown in Figures 11 and 12. The statistics of the prediction results are shown in Table I. The predicted and measured HCs were highly correlated with an r^2 of 0.995 and an RMSEEV of 0.0226 wt % for the FT-NIR PLS-R model and an r^2 of 0.996 and an RMSEEV of 0.0189 wt % for the ATR–FTIR PLS-R model. These results confirm that the rapid prediction of HC by the FT-NIR and ATR–FTIR PLS-R models is feasible.

CONCLUSIONS

The aim of this study was to analyze the feasibility of the HC determination of HS-oil samples by a combination of FT-NIR and ATR–FTIR with PLS-R models. The FT-NIR PLS-R and ATR–FTIR PLS-R models were successfully used to determine the HCs of the HS-oil samples, and this prevented pollution and time-consuming and troublesome issues, and the rapid measurement of HC was achieved. The validation results demonstrated that FT-NIR and ATR–FTIR spectroscopy combined with multivariate statistical methods were accurate and practical for the rapid analysis of the HCs of the HS-oil.

ACKNOWLEDGMENTS

The authors are grateful to Pengchao Si for his suggestion and the help of The Unscrambler.

REFERENCES

1. Feng, S. Y.; Zhang, J.; Li, M. J.; Zhu, Q. Z. In Silicone Polymer and Its Application; Feng, S. Y., Ed.; Chemical Industry: Beijing, **2004**; Chapter 16, p 393.
2. Stark, E.; Luchter, K.; Margoshes, M. *Appl. Spectrosc. Rev.* **1986**, *22*, 335.
3. Herschel, W. *Philos. Trans. R. Soc.* **1800**, *90*, 284.
4. Fernández-Ibañez, V.; Soldado, A.; Martínez-Fernández, A.; de la Roza-Delgado, B. *Food Chem.* **2009**, *113*, 629.
5. Kirsanov, D.; Mednova, O.; Vietoris, V.; Kilmartin, P. A.; Legin, A. *Talanta* **2012**, *90*, 109.
6. Liu, Y.; Ying, Y.; Yu, H.; Fu, X. *J. Agric. Food Chem.* **2006**,*54*, 2810.
7. Mouazen, A. M.; Maleki, M. R.; De Baerdemaeker, J.; Ramon, H. *Soil Tillage Res.* **2007**, *93*, 13.
8. Romera-Fernández, M.; Berrueta, L. A.; Garmón-Lobato, S.; Gallo, B.; Vicente, F.; Moreda, J. M. *Talanta* **2012**, *88*, 303.
9. Stefanov, I.; Baeten, V.; Abbas, O.; Vlaeminck, B.; De Baets, B.; Fievez, V. *J. Agric. Food Chem.* **2013**, *61*, 3403.
10. Fox, G. P.; O'Donnell, N. H.; Stewart, P. N.; Gleadow, R. M. *J. Agric. Food Chem.* **2012**, *60*, 6183.
11. Wu, D.; He, Y.; Shi, J.; Feng, S. *J. Agric. Food Chem.* **2009**, *57*, 1697.
12. Dupuy, N.; Galtier, O.; Ollivier, D.; Vanloot, P.; Artaud, J. *Anal. Chim. Acta* **2010**, *666*, 23.
13. Rambo, M. K. D.; Amorim, E. P.; Ferreira, M. M. C. *Anal. Chim. Acta* **2013**, *775*, 41.
14. Downey, G. *J. Near Infrared Spectrosc.* **1996**,*4*, 47.
15. Givens, D. I.; Deaville, E. R. *Aust. J. Agric. Res.* **1999**, *50*, 1131.
16. Prieto, N.; Roehe, R.; Lavín, P.; Batten, G.; Andrés, S. *Meat Sci.* **2009**, *83*, 175.
17. Tsuchikawa, S. *Appl. Spectrosc. Rev.* **2007**, *42*, 43.
18. Huang, H.; Yu, H.; Xu, H.; Ying, Y. *J. Food Eng.* **2008**, *87*, 303.
19. Kuligowski, J.; Cascant, M.; Garrigues, S.; de la Guardia, M. *Talanta* **2012**, *99*, 660.
20. Suárez, L.; García, R.; Riera, F. A.; Diez, M. A. *Talanta* **2013**, *115*, 652.
21. Awotwe-Otoo, D.; Zidan, A.; Rahman, Z.; Habib, M. *AAPS PharmSciTech* **2012**, *13*, 611.
22. Ulmschneider, M.; Pénigault, E. *Analusis* **2000**,*28*, 136.
23. Higgins, J. P.; Arrivo, S. M.; Thurau, G.; Green, R. L.; Bowen, W.; Lange, A.; Templeton, A. C.; Thomas, D. L.; Reed, R. A. *Anal. Chem.* **2003**, *75*, 1777.
24. Li, W.; Worosila, G. D.; Wang, W.; Mascaro, T. *J. Pharm. Sci.* **2005**, *94*, 2800.
25. Aske, N.; Kallevik, H.; Sjöblom, J. *Energy & Fuels* **2001**, *15*, 1304.
26. Balabin, R. M.; Safieva, R. Z. *Energy & Fuels* **2011**, *25*, 2373.
27. Cramer, J. A.; Morris, R. E.; Giordano, B.; Rose-Pehrsson, S. L. *Energy & Fuels* **2009**, *23*, 894.
28. Felizardo, P.; Baptista, P.; Menezes, J. C.; Correia, M. J. N. *Anal. Chim. Acta* **2007**, *595*, 107.
29. Costa, N.; Amaral, S.; Alvim, R.; Nogueira, M.; Schwanninger, M.; Rodrigues, J. *J. Appl. Polym. Sci.* **2013**, *128*, 498.
30. Alig, I.; Lellinger, D.; Agarwal, S.; Oehler, H. *React. Funct. Polym.* **2013**, *73*, 316.
31. Watanabe, S.; Dybal, J.; Tashiro, K.; Ozaki, Y. *Polymer* **2006**, *47*, 2010.
32. Darcos, V.; Monge, S.; Haddleton, D. M. *J. Polym. Sci. Part A: Polym. Chem.* **2004**, *42*, 4933.
33. Fontoura, J. M. R.; Santos, A. F.; Silva, F. M.; Lenzi, M. K.; Lima, E. L.; Pinto, J. C. *J. Appl. Polym. Sci.* **2003**, *90*, 1273.
34. Cherfi, A.; Fevotte, G.; Novat, C. *J. Appl. Polym. Sci.* **2002**, *85*, 2510.
35. Henriques, A.; Cruz, P.; Martins, J.; Ferra, J. M.; Magalhães, F. D.; Carvalho, L. H. *J. Appl. Polym. Sci.* **2012**, *124*, 2441.
36. Heigl, N.; Petter, C. H.; Rainer, M.; Najam-ul-Haq, M.; Vallant, R. M.; Bakry, R.; Bonn, G. K.; Huck, C. W. *J. Near Infrared Spectrosc.* **2007**, *15*, 269.
37. Lousberg, H. H. A.; Boelens, H. F. M.; Le Comte, E. P.; Hoefsloot, H. C. J.; Smilde, A. K. *J. Appl. Polym. Sci.* **2002**, *84*, 90.
38. Marengo, E.; Longo, V.; Robotti, E.; Bobba, M.; Gosetti, F.; Zerbinati, O.; Di Martino, S. *J. Appl. Polym. Sci.* **2008**, *109*, 3975.
39. Mauer, L. J.; Chernyshova, A. A.; Hiatt, A.; Deering, A.; Davis, R. *J. Agric. Food Chem.* **2009**, *57*, 3974.